

# Structure and Stability of ( $\alpha$ -CD)<sub>3</sub> Aggregate and OEG@( $\alpha$ -CD)<sub>3</sub> Pseudorotaxane in Aqueous Solution: A Molecular Dynamics Study

Cleber P. A. Anconi,<sup>\*,†</sup> Clebio S. Nascimento, Jr.,<sup>‡</sup> Wagner B. De Almeida,<sup>‡</sup> and Hélio F. Dos Santos<sup>†</sup>

*Núcleo de Estudos em Química Computacional (NEQC), Departamento de Química, ICE, Universidade Federal de Juiz de Fora (UFJF), Campus Universitário, Martelos, Juiz de Fora, MG 36036-330, Brazil, and Laboratório de Química Computacional e Modelagem Molecular (LQC-MM), Departamento de Química, ICEx, Universidade Federal de Minas Gerais (UFMG), Campus Universitário, Pampulha, Belo Horizonte, MG 31270-901, Brazil*

*Received: April 6, 2009; Revised Manuscript Received: June 2, 2009*

Empty linear associations accounting for three  $\alpha$ -CD units and their corresponding pseudorotaxanes have been studied by means of long length molecular dynamics (MD) simulations in a vacuum and in aqueous solution. Results from MD for empty sequences lead to a quite stable arrangement formed by three mutually perpendicular cyclodextrin (CD) units named here as 3P. In such a spatial arrangement, the van der Waals term in the force field is pronounced, accounting for almost 40% of the association energy, which ensures the noticeable stability of the 3P association even in aqueous media. In addition, it can be stated that only the presence of the oligomer forces the CD units to acquire an almost linear association. Mutually perpendicular-based arrangements are the most favorable spatial disposition in aqueous media. We believe this work is the first step toward a more ambitious study including very large CD sequences, aiming to understand the association process in aqueous solution at a molecular level.

## 1. Introduction

Cyclodextrin (CD)<sup>1</sup> is a cyclic oligomer of  $\alpha$ -D-glucose obtained by the action of certain enzymes on starch. Generally described as shallow truncated cones, this class of carbohydrate presents a hydrophobic cavity of different sizes, depending on the number of elementary glucose units, and two different rims, a wider (named head, H) containing all secondary hydroxyl groups and a narrower (named tail, T) containing all primary hydroxyl groups. There are three natural cyclodextrins readily available having six, seven, or eight glucose units named  $\alpha$ -CD,  $\beta$ -CD, and  $\gamma$ -CD, respectively. The applicability of CDs in supramolecular chemistry is closely related to its ability to form inclusion compounds with a wide range of guest molecules in aqueous solutions.<sup>2,3</sup> Due to its singular architecture, in the context of the supramolecular chemistry, CDs can be used as molecular reactors<sup>4–6</sup> or in molecular recognition processes,<sup>7–11</sup> being also the host molecule employed in the synthesis of novel materials such as molecular wires<sup>12–14</sup> and molecular nanotubes.<sup>15–18</sup> The encapsulating phenomena of high molecular weight compounds by CDs have been the subject of numerous investigations. The number of publications related to this host–guest branch has experienced a significant increase after the independent and pioneer works of Harada and Kamachi<sup>19</sup> and Wenz and Keller.<sup>20</sup> These research groups have proved unequivocally that CD units form inclusion compounds in high yields with distinct water-soluble polymers. According to the experimental findings, the inclusion of a polymeric chain in the CD channel is entropically unfavorable. The formation of the complexes is thought to be promoted by hydrogen bonds

between CDs.<sup>21–24</sup> In addition, the resulting supramolecular entity is often named pseudopolyrotaxane (PR).<sup>25</sup>

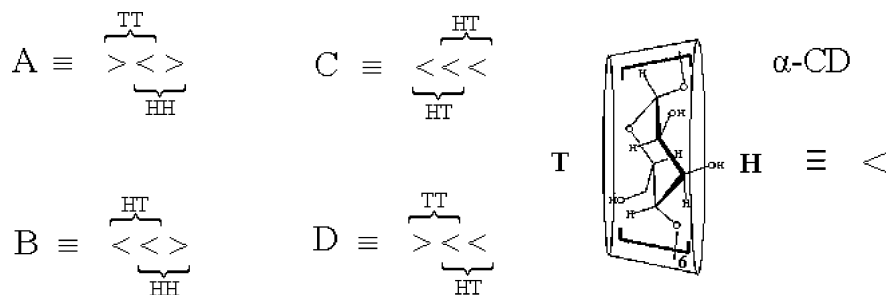
In sequential supramolecular structures such as pseudopolyrotaxanes, CDs can be assembled in different forms. For such a kind of compounds, the dimeric arrangement is usually assumed to be the smallest representative structure. In this sense, three possible isomers named head-to-head (HH), tail-to-tail (TT), or head-to-tail (HT), with alignments defined depending on how each CD rim is faced toward another, can be interpreted as the building blocks of such a class of novel materials. Ending capping pseudopolyrotaxanes give rise to polyrotaxanes (“molecular necklaces”) preserving the original associations formed in the threading process.<sup>26–29</sup> The condensation of CD threaded on a polymer chain with epichlorohydrin results in the formation of molecular tubes (MT).<sup>30,31</sup> Very recently, our research group<sup>32</sup> pointed out that the orientations of CD’s units in the molecular necklace play an important role in the synthesis of MT, which is certainly the most important CD pseudopolyrotaxane derivative. Despite the intensive efforts focused in this research field,<sup>2,15,17,33–35</sup> some fundamental questions are still unclear. One important aspect concerns the distinct stabilities of the three possible dimeric associations of CD’s unit being the HH form the most stable one. Usually, the HT association is classified as imperfection, but the TT association has been addressed as the most unstable association.<sup>36,37</sup> Nonetheless, it was found experimentally that TT represents 40% of the total possible associations in necklaces synthesized by the threading process,<sup>38</sup> clearly a self-assembly stage in the synthetic route. Thus, further studies are still necessary in order to assess the role played by cooperative effects and included polymers on the relative stability of small CD-based building blocks. In this context, the present paper deals with the structure and stability of distinct ( $\alpha$ -CD)<sub>3</sub> sequences possessing or not possessing an oligo(ethylene glycol) (OEG) chain in the cavity formed by the three

\* Corresponding author. E-mail: cleber@netuno.qui.ufmg.br. Fax: 55 32 3229 3314.

<sup>†</sup> Universidade Federal de Juiz de Fora (UFJF).

<sup>‡</sup> Universidade Federal de Minas Gerais (UFMG).

# SCHEME 1



$\alpha$ -CD units. Long molecular dynamics (MD) simulations in a vacuum and in aqueous media have been performed in order to provide reliable information concerning fundamental aspects of PR chemistry and aggregation phenomena in aqueous solution.

## 2. Theoretical Details

The  $\alpha$ -CD monomer used to obtain the starting geometries for the three possible dimeric associations, differing only in the positions of primary hydroxyl groups that can rotate freely, is equivalent to the structure expected to be predominant in aqueous media, determined previously by our research group.<sup>39</sup> The geometric parameters of the starting dimeric associations were estimated on the basis of the data previously determined in the gas phase for empty  $\alpha$ -CD associations.<sup>36</sup> The three dimers obtained were fully optimized at the semiempirical PM3 level of theory without any constraint. Afterward, the three optimized geometries obtained possessing all possible intermolecular hydrogen bonds ( $r_{\text{CM}} = 7.6, 8.2,$  and  $8.5 \text{ \AA}$  for HH, TT, and HT, respectively) were minimized using the AMBER\* force field<sup>40,41</sup> as implemented in the Macromodel package,<sup>42</sup> the software employed to perform the MD simulations in a vacuum. The trimers investigated in this work have been obtained using the parameters determined from the AMBER\* optimized dimers. All empty resulting structures have been submitted to minimization with the AMBER\* force field prior to performing the MD simulations in a vacuum.

From the analysis of the eight possible sequences formed with three CD units, only four arrangements are necessary, with the other four isomers being structurally degenerated. Those arrangements possessing three CD units have been identified by the capital letters A, B, C, and D, whose sequences are represented in Scheme 1. In order to obtain the [4]pseudorotaxane starting structures, a previously optimized OEG chain, comprising seven ethylene glycol units, has been included in the trimeric associations. The size of the polymeric chain that determines the molar ratio of ethylene glycol units to  $\alpha$ -CD has been chosen on the basis of theoretical and experimental<sup>43</sup> information. After the inclusion, the OEG chain has been rotated around the main axis of the molecule and the AMBER\* force field used in order to determine the most stable orientation. The global minimum for each arrangement was used as the starting geometry submitted to the MD simulations.

Molecular dynamics (MD) simulations in a vacuum were performed employing the AMBER\* force field considering each structure obtained by the preceding strategy. Cutoff radii for van der Waals and Coulombic electrostatic interactions were 8 and 20  $\text{\AA}$ , respectively. All C–H and O–H bond lengths were held fixed using the SHAKE<sup>44</sup> algorithm. All MD runs were started with an initial temperature of 5 K and warmed up to 50 K for 10 ps and then equilibrated for 100 ps. Subsequently, five similar consecutive molecular dynamics steps were executed. In each step, the structures were warmed up to 50 K

for 10 ps and equilibrated for 100 ps. All MD simulations performed in a vacuum, with a length of 10 ns, had a time step of 1.5 fs and were performed at 300 K.

Molecular dynamics simulations in aqueous media were carried out for empty dimeric and trimeric associations employing the GAFF (generalized AMBER force field) as implemented in the AMBER 10 package.<sup>45</sup> The atomic charges employed in the condensed phase simulations have been obtained from the BCC approach<sup>46</sup> through the aid of the *antechamber* software, an AMBER 10 accessory module. Within this approach, simple additive bond charge corrections (BCCs) are applied to AM1 atomic charges to produce AM1-BCC charges, which were parametrized to reproduce the HF/6-31G\* RESP charges. In the “RESP” procedure, the molecular structure is used to calculate a molecular electrostatic potential (MEP) on a three-dimensional grid that is exported into a specific program (RESP program) which is used to fit atom-centered charges to the MEP. In order to include explicit solvent molecules, the TIP3P water model has been chosen by means of a periodic solvent octahedric box. The parameter that determines the closest distance between any atom of the solute and the edge of the periodic box corresponds to 9.7, 9.7, and 10  $\text{\AA}$  for HH, TT, and HT, respectively, and 9.0, 8.6, 8.6, and 9.0  $\text{\AA}$  for the empty trimers A, B, C, and D, respectively. The average number of water molecules included was 1500 for empty sequences and 1660 for PRs. The same parameters determined for empty trimers have been used in order to construct the octahedric periodic box for the filled [4]pseudorotaxanes (the filled trimers). All systems including solute and solvent molecules have been fully optimized with GAFF prior to starting the aqueous MD simulation in order to avoid close contacts or problems with van der Waals (nonbond) and electrostatic interactions in the initial structures. The same warming up process employed in the simulations performed in a vacuum has been used in condensed phase simulations. In what concerns the thermodynamic conditions, an NVT ensemble has been used in the warming up process and an NPT ensemble in the production period with a simulation length of 5000 or 10000 ps in specific cases in order to discuss some fundamental aspects. A non-bonded cutoff of 10.0  $\text{\AA}$  has been employed for all simulations in solution.

In order to discuss the relative stability of the empty and filled trimeric  $\alpha$ -CD associations in aqueous media, representative snapshots collected along the trajectories have been treated employing the molecular mechanics/Poisson–Boltzmann surface area (MM-PBSA) methodology. Within this approach, the absolute energy in solution (AES) is determined in the MM-PBSA approach by the following scheme:

$$\text{AES} = E_{\text{gas}} + \Delta G_{\text{solv}} \quad (1)$$

With the right-hand terms in eq 1 defined as

$$E_{\text{gas}} = E_{\text{internal}}(\text{bond, angle, torsion}) + E_{\text{electrostatic}} + E_{\text{vdW}} \quad (2)$$

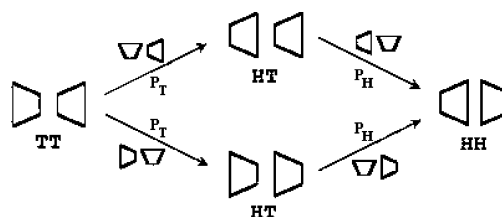
$$\Delta G_{\text{solv}} = \Delta G_{\text{PB}} + \Delta G_{\text{nonpolar}} \quad (3)$$

The molecular mechanics gas phase energy ( $E_{\text{gas}}$ ) describes both bonding and nonbonding interactions, eq 2. The bonding interactions are usually formulated as a strain energy that is zero at some ideal configuration of the atoms and describe how the energy increases as the ideal configuration is deformed. The internal term ( $E_{\text{internal}}$ ), that describes bonding interactions, corresponds to the summation of  $E_{\text{bond}}$ , a term associated with deformation of a bond from its standard equilibrium length,  $E_{\text{angle}}$ , a term associated with the deformation of an angle from its "normal" value, and  $E_{\text{torsion}}$ , a term associated with the tendency of dihedral angles to have a certain  $n$ -fold symmetry and to have minimum energy for the cis-, gauche-, or trans-conformation. In what concerns the nonbonding interactions, the  $E_{\text{electrostatic}}$  term describes the classical nonbonded electrostatic interactions of charge distributions, a potential that comprises the monopole–monopole interactions of atomic charges at a certain distance apart, and the van der Waals term ( $E_{\text{vdW}}$ ) that describes the repulsive forces keeping two nonbonded atoms apart at close range and the attractive force drawing them together at long range. The molecular mechanics gas phase energies ( $E_{\text{gas}}$ ) are determined with the *sander* program from the AMBER 10 package<sup>45</sup> using the same force field employed in the MD simulations performed in aqueous media. According to eq 3, the solvation free energies ( $\Delta G_{\text{solv}}$ ) are evaluated by summation of two contributions,  $\Delta G_{\text{PB}}$  and  $\Delta G_{\text{nonpolar}}$ . A numerical solver for the Poisson–Boltzmann (PB) method, as implemented in the *pbsa* program, included in the AMBER 10 package, gives the electrostatic contribution to the solvation free energy ( $\Delta G_{\text{PB}}$ ). Solvent-accessible-surface-area-dependent terms, also implemented in the AMBER 10 package,<sup>45</sup> give the nonpolar or hydrophobic contribution to the solvation free energy ( $\Delta G_{\text{nonpolar}}$ ).

### 3. Results and Discussion

**Structural Analysis.** For comparison and analysis, initially, the MD simulations for empty dimeric associations in a vacuum and in the condensed phase have been performed. In what concerns the dimeric associations, it has been well established<sup>37</sup> that the TT and HT associations are converted to the most stable HH in a vacuum. The change in orientation of those associations occurs in steps in which a perpendicular arrangement connects two distinct conformations. Along the MD simulations in a vacuum, those modifications of the original orientations have been observed, with two steps required in the conversion of TT into HH and only one step to achieve a HH from HT dimer. These processes are schematically represented in Scheme 2. In addition, two distinct forms for the intermediate species have been found, named here as  $P_{\text{H}}$  and  $P_{\text{T}}$ . The subscripts indicate the portion of the CD cavity of one CD unit (head or tail) that interacts with another CD unit, in a perpendicular arrangement, in this work represented by P. Interestingly, besides some conformational modifications along 10 ns, no orientation changes have been observed in the vacuum MD simulation performed for the empty HT starting association. Different from that observed for HH, an association that maintains its arrangement along the entire simulation, in the case of the HT structure, the number of hydrogen bonds, on average, is not sufficient enough to keep a single arrangement for a long time, at 300 K.

SCHEME 2



In a 30 ns length MD simulation, the HT association was found to exist until approximately 40% of the simulation length. Subsequently, the HT association changes its orientation, adopting an HH conformation, the average structure obtained at the end of this very long simulation. In the condensed phase, none of the dimeric association conserves its original parallel arrangement, as also pointed out by Jaime and co-workers.<sup>47</sup> In addition, the natural trend to convert all of the associations into the HH form has not been observed. In fact, the distinct associations tend to acquire a distorted perpendicular form in aqueous solution, favoring the solute...solvent hydrogen bonds.

In what concerns the trimeric association, based on the trajectories obtained along the MD simulations performed in a vacuum, the starting sequences can be divided into two groups, being the existence of an HH association, for A and B (see Scheme 1), the main characteristic employed to split the analysis. During the whole MD simulation for A and B empty starting sequences, the HH association was kept unaltered, in a vacuum. This behavior can be explained by the higher stability of the HH spatial arrangement. Nonetheless, the neighbor associations (TT for A and HT for B, see Scheme 1) do not maintain their original arrangements along the simulations, being converted to a perpendicular form (P). In the trajectory of the empty A sequence, the TT orientation has been changed along the simulation passing through the steps required to convert this association into HH form (see Scheme 2). A  $P_{\text{T}}$  arrangement has been initially obtained, and subsequently, this intermediate structure is converted into HT association. Thus, the sequence A is converted to B prior to reaching the equilibrium structure, characterized as  $P_{\text{H}}$ –HH. Focusing on the B starting structure, similar conversions have been observed; however, only one step is required to yield the final structure. The final  $P_{\text{H}}$ –HH structure is depicted in Figure 1a.

On the basis of the resulting average spatial arrangements obtained for A and B empty sequences in a vacuum, some fundamental aspects can be discussed. It is noticeable, for example, that the P spatial arrangement can be classified as an intermediate structure in the interconversion pathway. In fact, such a spatial arrangement is fundamentally a stationary point on the AMBER\* potential energy surface (PES), as attested by geometry optimization. In addition, according to a recent work developed by our research group in which hydrated  $\alpha$ -CD associations have been investigated,<sup>48</sup> the perpendicular arrangement was also identified as a stationary point on a quantum mechanical PES. In that previous work, it was pointed out that the interaction energy of the P association is considerable in the gas phase where the HH form has been identified as the most stable association at the BLYP/6-31G(d,p)/PM3 level of theory. This, in a certain way, explains the considerable stability of the P forms observed along the MD simulations performed in a vacuum, especially in what concerns the  $P_{\text{H}}$  arrangement for empty associations.

The results obtained in a vacuum for the second group of structures are very distinct. This group comprises the C and D sequences, which do not contain the HH association (see Scheme



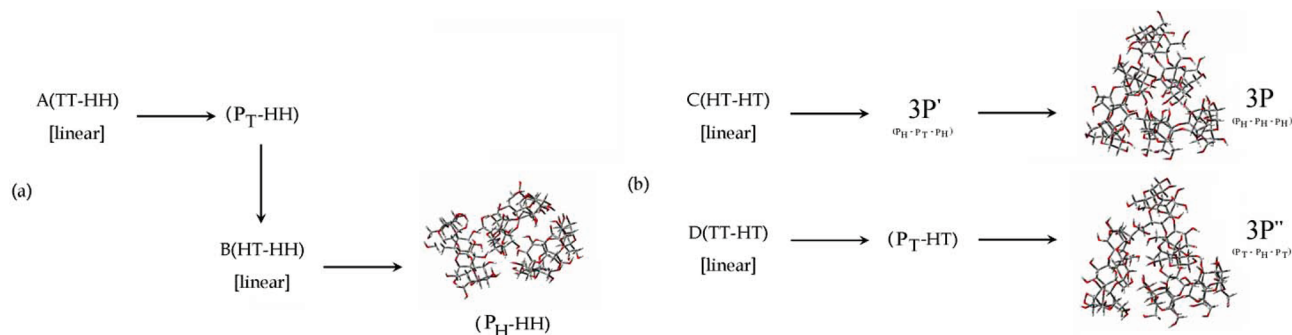


**Figure 1.** (a) Conversion of the linear A and B sequences into P<sub>H</sub>-HH arrangements. (b) Conversion of the linear C and D sequences into the 3P and 3P'' arrangements, respectively. It is noticeable that the 3P spatial arrangement resembles three P<sub>H</sub> associations and the resulting arrangement obtained from D resembles a P<sub>T</sub>-P<sub>H</sub>-P<sub>T</sub> association.

1). On the basis of the previous discussion for  $(\alpha\text{-CD})_2$ , the formation of the HH orientation from a HT association is the expected result for empty associations in a vacuum. Nonetheless, an interesting and new spatial arrangement has been obtained for  $(\alpha\text{-CD})_3$ . This arrangement is equivalent to three perpendicular associations, with the most stable form being 3P, built up by three P<sub>H</sub> forms. The 3P structure may also contain some P<sub>T</sub> associations, named in this work as 3P' or 3P'' when one or two P<sub>T</sub> associations have been identified, respectively. At the end of the MD simulations, the average 3P and 3P'' arrangements have been obtained from C and D empty sequences, respectively. Focusing on the C empty starting trimer, some sort of linearity has been detected for a considerable interval along the MD simulation, approximately 20% of the total length, which can be explained by the relative stability of the HT association. The subsequent step required in order to obtain a HH association (a P form) forces the CD units to acquire a nonlinear-based arrangement. Therefore, a significant modification in the spatial disposition of all CD units takes place, giving rise to a considerable stable 3P' arrangement at approximately 40% of the total length. As discussed previously in this work, along the simulation, the most stable form can be obtained by the conversion of P<sub>T</sub> into the P<sub>H</sub> form, in a vacuum. Thus, the 3P' association has been modified along the trajectory, resulting in a 3P association as an average spatial arrangement that was kept unaltered until the end of the simulation, as illustrated in Figure 1b. In what concerns the D empty sequence, a P<sub>T</sub> arrangement has been initially obtained from the TT association. Subsequently, the remaining HT dimer has been converted into a perpendicular form, resulting in a 3P'' association, as also illustrated in Figure 1b. The 3P'' has been identified at the end of 10 ns of simulation for the starting D sequence. As discussed, all conversions are in agreement with the steps indicated in Scheme 2.

In order to compare the stability of the P<sub>H</sub>-HH (Figure 1a) and 3P (Figure 1b) forms, the last structures obtained from the empty B and C sequences have been submitted as starting geometries to a 10 ns length MD simulation, in a vacuum. It is noticeable that no significant modification has been observed for both starting geometries. The number of hydrogen bonds has been determined for each structure collected and stored along the entire MD simulations. Therefore, the average value, named ANHB, has been evaluated. For those simulations, 5000 structures have been stored, and the average number of hydrogen bonds (ANHB) calculated for P<sub>H</sub>-HH and 3P corresponds to  $11 \pm 2$  and  $6 \pm 2$ , respectively. The difference in ANHB clearly is due to the existence of an HH association in the P<sub>H</sub>-HH arrangement. Subsequently, the 3P structure has been submitted to MD comprising in the warming up process the following

final temperatures: 350, 400, and 450 K. The 3P association maintained its original spatial arrangement in the MD simulation performed at 350 and 400 K. At 450 K, the 3P association is converted into P<sub>H</sub>-HH. However, after some time interval, P<sub>H</sub>-HH is converted again into 3P, characterizing a state of equilibrium between those forms at high temperature. These results suggest that the P<sub>H</sub>-HH  $\rightarrow$  3P process is kinetically controlled, with the former found as the thermodynamic product by the AMBER\* force field. Nonetheless, the results obtained also suggest that a very stable aggregate not possessing any HH association can be formed by CD units. In this aggregate, all of the individual molecules are assembled in a perpendicular arrangement to its neighbors.

In order to assess the role played by distinct force fields on the stability of 3P, the simulations were also performed with the GLYCAM\_06, parm99, GAFF, and MM3\* force fields. In all simulations performed, no significant modification was observed concerning the force fields available in the AMBER 10 package<sup>45</sup> (GLYCAM\_06, parm99, and GAFF). In what concerns the MM3\*, available with the Macromodel package,<sup>42</sup> the 3P arrangement was found to also be considerably stable but slightly distorted when compared to the other force field used. It is noticeable that even with MM3\* the 3P association was kept almost unaltered along the simulations (30 ns for this force field), although for much flexible molecules, such as large CDs, the results may be considerably distinct from GLYCAM and parm99.<sup>49</sup> Those results strongly support the main conclusion concerning the stability of the CD mutually perpendicular arrangement named 3P. It is noticeable that such a spatial arrangement, as the 3P association depicted in Figure 1b, is quite similar to crystal structure determinations for  $\alpha\text{-CD}$ .<sup>50–53</sup> Besides, in a recent paper, Li and co-workers<sup>54</sup> described tin complexes with  $\beta\text{-CD}$ , where three CDs coordinate to two Sn centers. The  $\beta\text{-CD}$  arrangement around the metals closely resembles our 3P structure.

The four  $(\alpha\text{-CD})_3$  sequences previously investigated in a vacuum have been submitted to MD simulations in aqueous media. The behavior of the trimeric association along the simulations performed in solution is quite interesting. In order to interpret the trajectories, the angle ( $\theta$ ) formed by the three CD centers of mass has been employed. In Figure 2, the corresponding  $\theta$  values have been depicted along the recorded trajectory for the four empty sequences investigated. From the analysis of Figure 2, it can be concluded that, after approximately 1 ns, the A and D empty sequences change their linear-based arrangements significantly. This fast interconversion might be due to the presence of the unstable TT association in both forms, which should be responsible for starting the process. The empty sequences B and C maintain approximately their

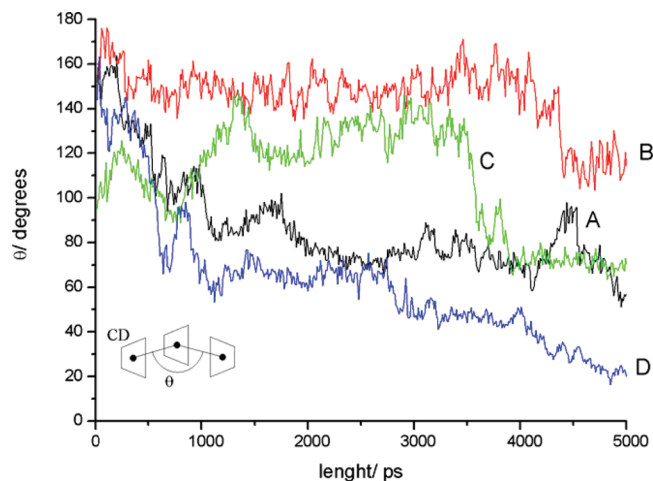


**Figure 2.** Angle between the centers of mass of the three CD units ( $\theta$ ), monitored along the MD simulations performed in aqueous media, at 300 K, for the three possible empty ( $\alpha$ -CD)<sub>3</sub> sequences.

linear arrangements up to  $\sim 4$  ns, when subtly they change their spatial arrangements. In the case of B, the equilibrium structure is closely related to P<sub>T</sub>-HH and for C the final geometry resembles the 3P structure. Thus, from previous analysis, the existence of 3P spatial arrangement in solution cannot be discarded. In fact, this association formed preferentially from HT sequences may help to understand the considerable small HT population determined experimentally, fundamentally bearing in mind that the 3P arrangement, in a certain way, does not favor the inclusion of an OEG chain. Eventually, some junctions in the so-called polyCD<sup>55</sup> have to be identified as HT associations, this because the HT existence has been undoubtedly detected in  $\alpha$ -CD PRs.<sup>38</sup>

On the basis of the previous discussion concerning the comparison between the stabilities of the 3P and P<sub>H</sub>-HH arrangements in a vacuum, those structures have been submitted as starting points to simulations in aqueous media, in which the  $\theta$  parameter has been monitored along the trajectories. The results have been depicted in Figure 3a. From the analysis of that figure, it can be observed that the 3P arrangement was kept almost unaltered along 5 ns of simulation in aqueous solution, with average  $\theta \sim 60^\circ$ . Therefore, the 3P form is a very stable association in aqueous media. For the P<sub>H</sub>-HH arrangement, a long length MD simulation has been performed and the natural trend to decrease the  $\theta$  parameter for trimeric associations in aqueous solution can be observed. Therefore, as indicated by a circle in Figure 3a after the formation of a 3P arrangement, the  $\theta$  parameter tends to increase, indicating a state of equilibrium between those spatial arrangements, as identified in high temperature vacuum simulations. Some representative average structures are also showed in Figure 3a, supporting the discussion concerning such equilibrium. Furthermore, the root-mean-square-deviation (rmsd) plot depicted in Figure 3b attests indubitably the stability of the 3P arrangement in aqueous solution. This behavior seems to be general for larger CDs, as also found recently by us for  $\beta$ -CD (unpublished results). However, a more systematic theoretical study has to be made concerning the larger CD aggregation in aqueous media.

As described in the methodology section, vacuum MD simulations have been carried out prior to the inclusion of the solvent effect for the four small pseudorotaxanes (PRs). In what concerns the vacuum trajectories, the [4]pseudorotaxanes OEG@A and OEG@B have been converted to [3]pseudorotaxanes. Therefore, for both filled systems, one  $\alpha$ -CD unit leaves the

supramolecular structure. Nonetheless, the HH association was kept unaltered and the OEG chain was included in the cavity formed by this stable association. The [4]pseudorotaxane status has been conserved until approximately 40% of the simulation length for A and 90% for B filled sequences. The formation of a P arrangement by the leaving CD unit was also observed where the OEG@HH association was kept unaltered. Therefore, the P<sub>H</sub>-HH and P<sub>T</sub>-HH has been identified at the end of the trajectories, with the polymer included in the portion of the aggregate formed by the HH association. In fact, the polymeric chain included tends to promote the intermolecular interaction between CD hydroxyl groups, which results in a maintenance of the [4]pseudorotaxane form, with the presence of the oligomer playing a role in the formation of hydrogen bond interactions. This feature explains the increase in the average potential energy detected for the filled associations when one CD unit leaves the supramolecular system to form the P association (result not shown). Focusing on the C and D filled sequences, no CD unit leaves the [4]pseudorotaxane systems along the whole MD simulation performed in a vacuum. In this respect, the existence of a TT association at the end of the simulation, for the D [4]pseudorotaxane, suggests that, for filled sequences comprising more than two CD units, the stability promoted by the included polymeric chain will allow the maintenance of every possible sequence formed in the self-assembly process.

As mentioned, simulations in aqueous media have been performed for all starting [4]pseudorotaxanes. The  $\theta$  parameter has also been used in order to clarify the results obtained. Along the whole MD simulations, all systems maintain their [4]pseudorotaxane status. In addition, the structures was kept in an almost linear form (see Figure 4), as can be concluded by the analysis of the average  $\theta$  parameter that corresponds to  $151 \pm 10$ ,  $146 \pm 11$ ,  $148 \pm 10$ , and  $159 \pm 70$  for OEG@A, OEG@B, OEG@C, and OEG@D, respectively. In fact, the  $\theta$  value is close to 180 only at low temperatures, which explains the average values. Clearly, the stabilization has been assured by the presence of the polymeric chain that promotes the hydrogen bonding between neighboring cyclodextrin rings. Due to the relative stability of mutually perpendicular form, it can be stated that the usual CD pair identification (HH, TT, or HT) will be applicable only for filled supramolecular assemblies, at least in dilute aqueous media, the simulation condition employed within this work. Therefore, only the presence of the oligomer will force  $\alpha$ -CD rings to acquire a sequential linear-based arrangement. Every possible pair sequence will be stabilized by the polymeric chain, and empty association in aqueous solution will resemble a P form.

In addition, a fundamental question still composes the scenario concerning the PR formation. If any filled sequence is stabilized in aqueous solutions, how to explain the HT small percentage (20%) detected in PR synthesized by Harada's procedure? Mutually perpendicular arrangements such as 3P, obtained under vacuum conditions from a system comprising only HT associations, can disfavor the formation of such a kind of association? The HT low percentage seems to be closely related to the balance concerning the time required for the formation of a particular association, the time required to modify a CD unit orientation, and the time necessary for the formation of a particular PR, assuming the formation of the polyCD prior to the inclusion phenomena, as pointed out by Lo Nostro and co-workers.<sup>55</sup> Theoretically, in order to investigate those dependencies, the species have to be accommodated randomly or in a predefined position in an adequate solvent box, in which a relatively long MD simulation will be performed. Additionally,

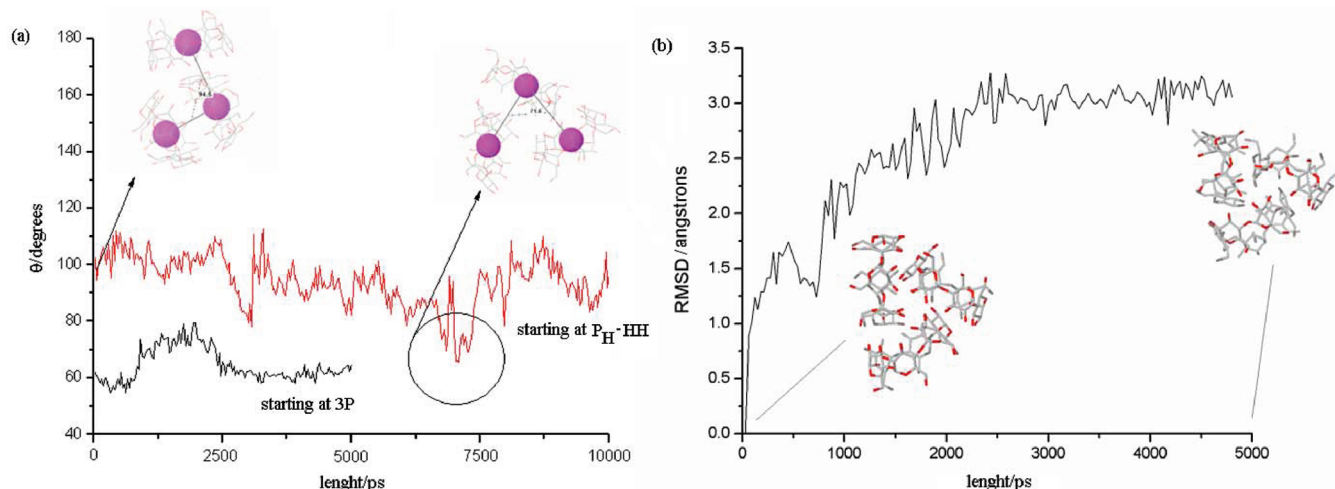


**Figure 3.** (a) Angle between the centers of mass of the three CD units ( $\theta$ ), monitored along the MD simulations performed in aqueous media, at 300 K, for the 3P and  $P_H$ -HH starting structures. Some representative average structures have been depicted showing the equilibrium established in aqueous media between the mentioned arrangements. (b) RMSD plot showing the 3P maintenance along the simulation performed in aqueous media for empty  $\alpha$ -CD.

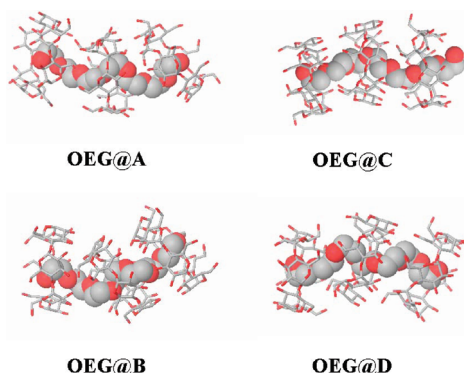


**Figure 4.** Final [4]pseudorotaxanes obtained at the end of 5 ns MD simulations performed in aqueous solutions. The water molecules have been removed for matter of clarity.

some 3P arrangements should be accommodated close to some polymeric chain, in aqueous solution, in order to discuss the PR formation in which the CDs are arranged in the most stable CD trimeric association, the 3P form, bearing in mind that 3P forms probably cannot act as hosts for filled arrangements. Therefore, the inclusion phenomena have to be observed along the simulations in order to study the time scales mentioned. This was not the main goal of the present work in which the species have been studied before and after the inclusion. In fact, the aqueous solution stability of the precursors and products discussed in the present work provides valuable information on the subsequent time scale study, a theoretical approach in which our group is also engaged.

**Relative Stability Analysis.** The energetic analysis carried out here was based on the MM-PBSA methodology, which accounts for contributions represented in eqs 1–3. It is important to make it clear that this is a sequential approach where a MD simulation in aqueous solution with explicit solvent molecules is first performed and, then, the resulting solute structures are selected and further used to calculate the energy contribution included in eqs 1–3. The gas phase energy is calculated using the GAFF force field and the solvation energy is obtained from the continuum solvation model based on Poisson–Boltzmann/surface area (PB/SA) approach.

In what concerns the stability of the systems studied, the previous structural analysis (Figures 2 and 3a) clearly showed

that a linear-based arrangement is not stable. The equilibrium structures obtained from A, C, and D showed  $\theta \sim 20$ – $60^\circ$ , which is consistent with a 3P-like arrangement. In the case of the B trajectory, the final structure presented averaged  $\theta \sim 100^\circ$  characterizing a kind of  $P_H$ -HH association. The MD simulations starting from 3P or  $P_H$ -HH did not change structure significantly throughout the whole trajectories, as shown in Figure 3a. In order to get insight on the driving forces for these interconversion processes, the isomer C was chosen as a representative for further analysis. A set of 1000 snapshots have been collected along the 10 ns MD trajectory in order to access the changes in the total gas phase energy,  $E_{\text{gas}}$  (see the Supporting Information). According to the contribution plots to  $E_{\text{gas}}$ , the  $E_{\text{electrostatic}}$  and  $E_{\text{vdw}}$  terms are more sensitive to the conversion of the linear-based form into a 3P-like arrangement. The  $E_{\text{internal}}$  term does not change significantly along the MD simulation performed in aqueous solution. This observation is supported by the average gas phase energy difference ( $\Delta E_{\text{gas}}$ ) evaluated from the structures (snapshots) collected along the MD runs performed for the 3P starting association and the free  $\alpha$ -CD, without explicit solvent molecules. The formation process,  $3\alpha\text{-CD}_{\text{FREE}} \rightarrow 3\text{P}$ , implies in a  $\Delta E_{\text{gas}}$  corresponding to  $-103 \text{ kcal}\cdot\text{mol}^{-1}$  being  $-71 \text{ kcal}\cdot\text{mol}^{-1}$  from  $\Delta E_{\text{electrostatic}}$ ,  $-44 \text{ kcal}\cdot\text{mol}^{-1}$  from  $\Delta E_{\text{vdw}}$ , and  $+12 \text{ kcal}\cdot\text{mol}^{-1}$  from  $\Delta E_{\text{internal}}$ . Therefore,  $\Delta E_{\text{electrostatic}}$  and  $\Delta E_{\text{vdw}}$  are the major contributions to the stabilization of the 3P association.

In order to discuss the relative stability of the empty and filled ( $\alpha$ -CD)<sub>3</sub> associations in the gas phase and aqueous media, snapshots collected along the trajectories of the studied systems have been analyzed. In the present work, 555 frames were used to calculate the average values given in Table 1. First, analyzing the gas phase energy, it can be seen from Table 1 that the 3P arrangement corresponds to the most stable empty association (last column). The main result concerning the empty sequences is related to the C starting arrangement. Despite the modification of the relative orientation observed for all empty sequences (see Figure 2), the C arrangement produces the most stable average structures along the simulations of the four sequences investigated ( $\Delta E_{\text{gas}} = 10.9 \text{ kcal}\cdot\text{mol}^{-1}$ ). This can be understood bearing in mind that in the vacuum simulation, the 3P arrangement has been obtained from that empty sequence, which is also the case in the aqueous simulation, as indicated by the  $\theta$  parameter in



**TABLE 1: Absolute Energy in Solution (AES), Gas Energy ( $E_{\text{gas}}$ ), and the Corresponding Relative Quantities, in  $\text{kcal}\cdot\text{mol}^{-1}$ , for All Empty and Filled Trimeric Species Studied**

species	AES <sup>a</sup>	$\Delta\text{AES}$	$E_{\text{gas}}$ <sup>b</sup>	$\Delta E_{\text{gas}}$
A	877.0	1.5	1206.0	42.0
B	883.8	8.2	1182.8	18.9
C	882.9	7.4	1174.8	10.9
D	875.5	0.0	1229.3	65.4
3P	901.7	26.2	1163.9	0.0
P <sub>H</sub> -HH	904.7	29.2	1186.4	22.5
OEG@A	952.7	12.1	1223.0	5.3
OEG@B	955.6	15.0	1217.7	0.0
OEG@C	952.4	11.8	1226.7	9.0
OEG@D	940.6	0.0	1222.4	4.7

<sup>a</sup> AES =  $E_{\text{gas}}$  +  $\Delta G_{\text{solv}}$ . <sup>b</sup>  $E_{\text{gas}}$  =  $E_{\text{internal}}(\text{bond, angle, torsion}) + E_{\text{electrostatic}} + E_{\text{vdW}}$ .

Figure 2. In what concerns the PRs, small differences have been evaluated, as can be seen from Table 1. It is interesting to note that the most unfavorable PR is formed by a sequence comprising only HT associations, the OEG@C structure. This is a reasonable result bearing in mind the experimental findings that indicate a small population of HT associations in PRs.

By analyzing the values in aqueous solution, we observed distinct trends for the stability order. The  $\Delta\text{AES}$  values in Table 1 indicate that the 3P association ( $\Delta\text{AES} = +26.2 \text{ kcal}\cdot\text{mol}^{-1}$ ) and the P<sub>H</sub>-HH ( $\Delta\text{AES} = +29.2 \text{ kcal}\cdot\text{mol}^{-1}$ ) are the most unfavorable spatial arrangements in aqueous solution, with the average association from D being the most stable form. In fact, from the relative energy values, it can be said that the equilibrium structures found from every initial linear arrangement (A, B, C, or D) are degenerated in aqueous solution. It is worth mentioning that the local spatial arrangements, defined by the  $\theta$  parameter in Figure 2, are distinct for every average structure. Nonetheless, the overall arrangements given by the average radius of gyration ( $R_g$ ) are similar, with values ranging from 7.4 to 9.4 Å, with the highest value found for D (9.4 Å) and the lowest for the 3P (7.4 Å) structure, where in the latter the CD units are more tightly bound. It is also interesting to notice that the  $R_g$  value predicted for the structure C (8.0 Å) is smaller than the predicted values for A, B, and D, being closer to those obtained for 3P, indicating a structural relationship between these forms. The free energy of solvation ( $\Delta G_{\text{solv}}$ ) of the 3P arrangement ( $-262.2 \text{ kcal}\cdot\text{mol}^{-1}$ ), as determined by the MM-PBSA approach, is significantly smaller, in absolute value, than the values evaluated for the four empty associations investigated ( $-353.8$  to  $-291.9 \text{ kcal}\cdot\text{mol}^{-1}$ ). The  $\Delta G_{\text{solv}}$  value found for 3P is close to the quantities evaluated for the four PRs that correspond to  $-270.3$ ,  $-262.1$ ,  $-274.3$ , and  $-281.8 \text{ kcal}\cdot\text{mol}^{-1}$  for A, B, C, and D filled sequences, respectively. The major contribution to  $\Delta G_{\text{solv}}$  is due to the electrostatic term ( $\Delta G_{\text{PB}}$ ); however, it is difficult to evaluate how accurately continuum methods may in principle be able to represent solvation. The high solvation energy for those structures obtained from A, B, C, and D in aqueous solution is in some way expected. Starting from linear arrangements, the aggregates like 3P and P<sub>H</sub>-HH are formed. However, in aqueous solution, the individual CDs are involved in many solute-solvent hydrogen bonds, which are responsible for distorting the final geometries. Thus, these aggregates are supposed to be more polar, which justify in part the higher solvation energy within the continuum model. It is interesting to note that it does not happen when the MD simulations are performed for the tight 3P or P<sub>H</sub>-HH aggregates, which is due in great part to the

cooperative van der Waals forces involved in the P arrangements. A more systematic way to account for the solvent effect on energy by means of MM-PBSA should include some explicit water molecules (for instance, the first solvation shell) before calculating the solvation energy. In the case of PR stability in aqueous solution, the arrangement D was found slightly more stable. However, as found in the gas phase, the relative energies in solution are small, indicating that all OEG@( $\alpha$ -CD)<sub>3</sub> arrangements are equally probable. Finally, in order to undoubtedly evaluate the dimeric relative stability of the associations named HH, HT, and TT in the PRs, in aqueous media, structures possessing a considerable number of CD units (say 15  $\alpha$ -CD) have to be investigated in long MD simulations in order to amplify the effect of the stabilization promoted by a particular set of dimeric associations. Our group is already engaged in such theoretical investigation.

#### 4. Conclusions

On the basis of long MD simulations carried out in a vacuum and in aqueous solution, some fundamental aspects concerning the stability of small aggregates, ( $\alpha$ -CD)<sub>3</sub>, and  $\alpha$ -CD-based pseudorotaxanes, OEG@( $\alpha$ -CD)<sub>3</sub>, have been discussed in this work. The main findings suggest the following conclusions:

- (1) A new quite stable aggregate not possessing any head-to-head (HH) association can be formed by  $\alpha$ -CD units in aqueous solution. In this aggregate, named 3P, all of the individual molecules are assembled in a perpendicular arrangement to its neighbors. This seems to be a general conclusion for larger cyclodextrins, such as  $\beta$ - and  $\gamma$ -CD.
- (2) Only the presence of the oligomer will force  $\alpha$ -CD rings to acquire a sequential linear-based arrangement in which every possible pair sequence will be stabilized by the polymeric chain.
- (3) Empty association in aqueous solution will resemble a perpendicular (P)-based spatial arrangement.

**Acknowledgment.** The authors would like to thank the Brazilian agencies CNPq (Conselho Nacional de Desenvolvimento Científico e Tecnológico) and FAPEMIG (Fundação de Amparo à Pesquisa do Estado de Minas Gerais) for financial support. This work was also partially supported by the projects PRONEX-FAPEMIG/EDT-526/07 and FAPEMIG/APQ-00498/08.

**Supporting Information Available:** Gas phase total energy and their contributions evaluated for the C empty sequence snapshots collected along MD simulations and root-mean-square-deviation plots (rmsd plots) for vacuum simulations performed with AMBER\*, MM3\*, GAFF, GLYCAM\_06, and parm99 force fields, for the 3P starting arrangement. This material is available free of charge via the Internet at <http://pubs.acs.org>.

#### References and Notes

- (1) Szejtli, J. *Chem. Rev.* **1998**, *98*, 1743–1753.
- (2) Harada, A. *Acc. Chem. Res.* **2001**, *34*, 456–464.
- (3) Connors, K. A. *Chem. Rev.* **1997**, *97*, 1325–1357.
- (4) Blenke, C.; Da Silva, V. J.; Junqueira, G. M. A.; De Almeida, W. B.; Dos Santos, H. F. *THEOCHEM* **2007**, *809*, 95–102.
- (5) Barr, L.; Dumanski, P. G.; Easton, C. J.; Harper, J. B.; Lee, K.; Lincoln, S. F.; Meyer, A. G.; Simpson, J. S. *J. Inclusion Phenom. Macrocyclic Chem.* **2004**, *50*, 19–24.
- (6) Dumanski, P. G.; Easton, C. J.; Lincoln, S. F.; Simpson, J. S. *Aust. J. Chem.* **2003**, *56*, 1107–1111.
- (7) Castro, E. A.; Barbiric, D. A. J.; Nascimento, C. S.; De Almeida, W. B.; Dos Santos, H. F.; Coscarello, E. *Mol. Simul.* **2006**, *32*, 623–631.

- (8) Dodziuk, H.; Ejchart, A.; Lukin, O.; Vysotsky, M. O. *J. Org. Chem.* **1999**, *64*, 1503–1507.
- (9) Dodziuk, H.; Kozminski, W.; Ejchart, A. *Chirality* **2004**, *16*, 90–105.
- (10) Lipkowitz, K. B.; Raghothama, S.; Yang, J. *J. Am. Chem. Soc.* **1992**, *114*, 1554–1562.
- (11) Liu, Y.; Han, B. H.; Sun, S. X.; Wada, T.; Inoue, Y. *J. Org. Chem.* **1999**, *64*, 1487–1493.
- (12) Shimomura, T.; Akai, T.; Abe, T.; Ito, K. *J. Chem. Phys.* **2002**, *116*, 1753–1756.
- (13) Yoshida, K.; Shimomura, T.; Ito, K.; Hayakawa, R. *Langmuir* **1999**, *15*, 910–913.
- (14) Bergamini, J. F.; Lagrost, C.; Ching, K. I. C.; Jouini, M.; Lacroix, J. C.; Aeiyaich, S.; Lacaze, P. C. *Synth. Met.* **1999**, *102*, 1538–1539.
- (15) Ikeda, T.; Hirota, E.; Qoya, T.; Yui, N. *Langmuir* **2001**, *17*, 234–238.
- (16) Ikeda, T.; Lee, W. K.; Ooya, T.; Yui, N. *J. Phys. Chem. B* **2003**, *107*, 14–19.
- (17) Ikeda, T.; Ooya, T.; Yui, N. *Polym. Adv. Technol.* **2000**, *11*, 830–836.
- (18) Li, G.; McGown, L. B. *Science* **1994**, *264*, 249–251.
- (19) Harada, A.; Kamachi, M. *Macromolecules* **1990**, *23*, 2821–2823.
- (20) Wenz, G.; Vonderbey, E.; Schmidt, L. *Angew. Chem., Int. Ed. Engl.* **1992**, *31*, 783–785.
- (21) Komiyama, M.; Miyake, K.; Sumaoka, J.; Harada, A.; Shigekawa, H. *Abstr. Pap. Am. Chem. Soc.* **1999**, *217*, U487.
- (22) Harada, A.; Li, J.; Suzuki, S.; Kamachi, M. *Macromolecules* **1993**, *26*, 5267–5268.
- (23) Harada, A.; Li, J.; Kamachi, M. *Macromolecules* **1994**, *27*, 4538–4543.
- (24) Harada, A.; Li, J.; Kamachi, M. *Macromolecules* **1993**, *26*, 5698–5703.
- (25) Nepogodiev, S. A.; Stoddart, J. F. *Chem. Rev.* **1998**, *98*, 1959–1976.
- (26) Wenz, G.; Han, B. H.; Muller, A. *Chem. Rev.* **2006**, *106*, 782–817.
- (27) Rekharsky, M. V.; Inoue, Y. *Chem. Rev.* **1998**, *98*, 1875–1917.
- (28) Harada, A.; Suzuki, S.; Okada, M.; Kamachi, M. *Macromolecules* **1996**, *29*, 5611–5614.
- (29) Harada, A.; Li, J.; Kamachi, M. *Nature* **1992**, *356*, 325–327.
- (30) Harada, A.; Li, J.; Kamachi, M. *Nature* **1993**, *364*, 516–518.
- (31) Samitsu, S.; Araki, J.; Shimomura, T.; Ito, K. *Macromolecules* **2008**, *41*, 5385–5392.
- (32) Anconi, C. P. A.; Nascimento, C. S.; De Almeida, W. B.; Dos Santos, H. F. *J. Inclusion Phenom. Macrocyclic Chem.* **2008**, *60*, 25–33.
- (33) Rusa, C. C.; Fox, J.; Tonelli, A. E. *Macromolecules* **2003**, *36*, 2742–2747.
- (34) Okumura, Y.; Ito, K.; Hayakawa, R. *Polym. Adv. Technol.* **2000**, *11*, 815–819.
- (35) Fleury, G.; Brochon, C.; Schlatter, G.; Bonnet, G.; Lapp, A.; Hadzioannou, G. *Soft Matter* **2005**, *1*, 378–385.
- (36) Anconi, C. P. A.; Nascimento, C. S.; De Almeida, W. B.; Dos Santos, H. F. *J. Braz. Chem. Soc.* **2008**, *19*, 1033–1040.
- (37) Bonnet, P.; Jaime, C.; Morin-Allory, L. *J. Org. Chem.* **2001**, *66*, 689–692.
- (38) Miyake, K.; Yasuda, S.; Harada, A.; Sumaoka, J.; Komiyama, M.; Shigekawa, H. *J. Am. Chem. Soc.* **2003**, *125*, 5080–5085.
- (39) Anconi, C. P. A.; Nascimento, C. S.; Fedoce-Lopes, J.; Dos Santos, H. F.; De Almeida, W. B. *J. Phys. Chem. A* **2007**, *111*, 12127–12135.
- (40) Weiner, S. J.; Kollman, P. A.; Nguyen, D. T.; Case, D. A. *J. Comput. Chem.* **1986**, *7*, 230–252.
- (41) Weiner, S. J.; Kollman, P. A.; Case, D. A.; Singh, U. C.; Ghio, C.; Alagona, G.; Profeta, S.; Weiner, P. *J. Am. Chem. Soc.* **1984**, *106*, 765–784.
- (42) Mohamadi, F.; Richards, N. G. J.; Guida, W. C.; Liskamp, R.; Lipton, M.; Caufield, C.; Chang, G.; Hendrickson, T.; Still, W. C. *J. Comput. Chem.* **1990**, *11*, 440–467.
- (43) Harada, A. *Supramol. Sci.* **1996**, *3*, 19–23.
- (44) Ryckaert, J. P. *Mol. Phys.* **1985**, *55*, 549–556.
- (45) Case, D. A. D.; Cheatham, T. A.; Simmerling, C. L.; Wang, J.; Duke, R. E.; Luo, R.; Crowley, M.; Walker, R. C.; Zhang, W.; Merz, K. M.; Wang, B.; Hayik, S.; Roitberg, A.; Seabra, G.; Kolossváry, I.; Wong, K. F.; Paesani, F.; Vanicek, J.; Wu, X.; Bronzell, S. R.; Steinbrecher, T.; Gohlke, H.; Yang, L.; Tan, C.; Mongan, J.; Hornak, V.; Cui, G.; Mathews, D. H.; Seetin, M. G.; Sagui, C.; Babin, V.; Kollman, P. A. *AMBER 10*; University of California, San Francisco: San Francisco, CA, 2008.
- (46) Jakalian, A.; Jack, D. B.; Bayly, C. I. *J. Comput. Chem.* **2002**, *23*, 1623–1641.
- (47) Bonnet, P.; Jaime, C.; Morin-Allory, L. *J. Org. Chem.* **2002**, *67*, 8602–8609.
- (48) Nascimento, C. S.; Anconi, C. P. A.; Dos Santos, H. F.; De Almeida, W. B. *J. Phys. Chem. A* **2005**, *109*, 3209–3219.
- (49) Maestre, I.; Bea, I.; Ivanov, P. M.; Jaime, C. *Theor. Chem. Acc.* **2007**, *117*, 85–97.
- (50) Manor, P. C.; Saenger, W. *J. Am. Chem. Soc.* **1974**, *96*, 3630–3639.
- (51) Klar, B.; Hingerty, B.; Saenger, W. *Acta Crystallogr., Sect. B* **1980**, *36*, 1154–1165.
- (52) Chacko, K. K.; Saenger, W. *J. Am. Chem. Soc.* **1981**, *103*, 1708–1715.
- (53) Lindner, K.; Saenger, W. *Acta Crystallogr., Sect. B* **1982**, *38*, 203–210.
- (54) Li, S. L.; Lan, Y. Q.; Ma, J. F.; Yang, J.; Zhang, M.; Su, Z. M. *Inorg. Chem.* **2008**, *47*, 2931–2933.
- (55) Lo Nostro, P.; Giustini, L.; Fratini, E.; Ninham, B. W.; Ridi, F.; Baglioni, P. *J. Phys. Chem. B* **2008**, *112*, 1071–1081.

JP903166E